

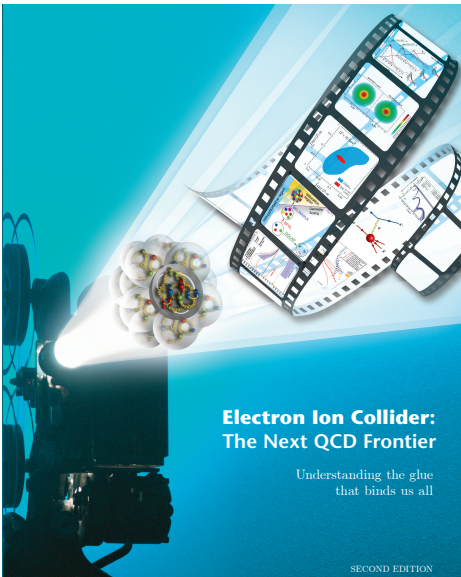
Diffractive Vector Meson and Dijet production from CGC at EIC

Heikki Mäntysaari

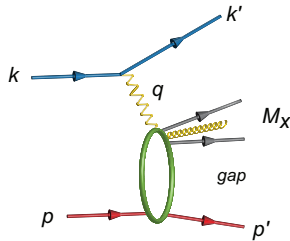
University of Jyväskylä, Department of Physics
Finland

September 25, 2019 / Physics and Detector Requirements at Zero-Degree of Colliders

Diffraction and the EIC microscope



Production of meson / dijet with a rapidity gap

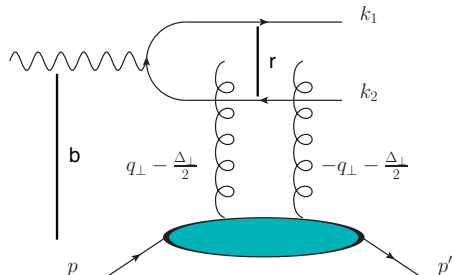


Advantages of diffraction

- (At least) 2-gluon exchange \Rightarrow sensitivity
- Measure $t \Rightarrow$ access to geometry

This talk: physics at small x (and small[ish] $|t|$)

Diffraction at high energy



$$\mathcal{A}^{\gamma^* p \rightarrow J/\Psi p} \sim \int d^2r d^2b e^{ib \cdot \Delta} \Psi^* \Psi(r, b, x_p) N(r, b, x_p)$$

High energy factorization

- ① $\gamma \rightarrow q + \bar{q}$ (photon wave function Ψ)
- ② Dipole-target interaction (dipole amplitude N)
- ③ $q + \bar{q} \rightarrow J/\Psi, \rho, \dots$ (J/Ψ wave function)
or $q + \bar{q} \rightarrow \text{dijet}$

Target remains intact (Good-Walker picture)

$$\frac{d\sigma}{dt} \sim |\langle \mathcal{A} \rangle|^2$$

Note: $N \sim xg$, so $\sigma \sim \text{gluon}^2$
+ access to geometry: $t \leftrightarrow b$ Fourier transform

Advantage of CGC: unified framework to describe inclusive and diffractive scattering

Incoherent diffraction = target dissociation

Incoherent cross section

- Target final state $|f\rangle \neq$ initial state $|i\rangle$
- Rapidity gap between J/Ψ and target remnants

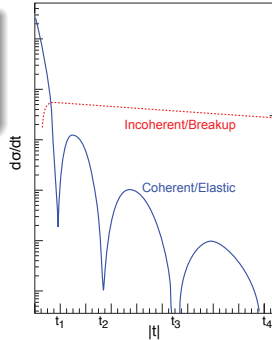
$$\begin{aligned}\sigma_{\text{incoherent}} &\sim \sum_{f \neq i} |\langle f | \mathcal{A} | i \rangle|^2 \\ &= \sum_f \langle i | \mathcal{A} | f \rangle^\dagger \langle f | \mathcal{A} | i \rangle - \langle i | \mathcal{A} | i \rangle^\dagger \langle i | \mathcal{A} | i \rangle\end{aligned}$$

Average over initial states:

$$\sigma_{\text{incoherent}} \sim \langle |\mathcal{A}|^2 \rangle_\Omega - |\langle \mathcal{A} \rangle_\Omega|^2$$

Incoherent cross section = variance of $\mathcal{A}^{\gamma^* A \rightarrow V A}$

- Measures the amount of event-by-event fluctuations in target configurations Ω



Miettinen, Pumpkin, PRD 18, 1978, Caldwell,
Kowalski, Phys.Rev. C81 (2010) 025203

Experimental separation:
intact/dissociated
proton/nucleus?

Applications of J/Ψ production 1: saturation (coherent photoproduction)

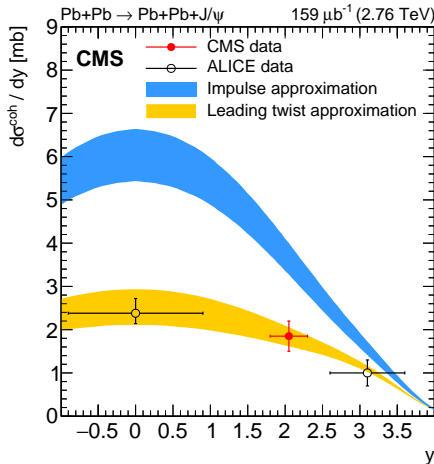
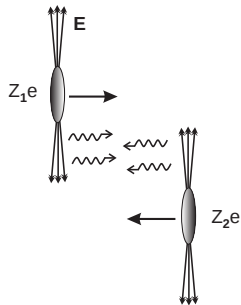
- Enhance saturation effects:

$$Q_{s,A}^2 \sim A^{1/3} x^{-\lambda}$$

(increasing A cheaper than decreasing x)

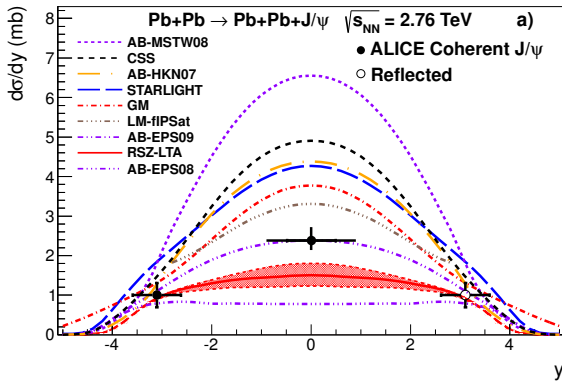
- Varying A at the EIC \Rightarrow different Q_s^2

Already data from UPCs ($x \sim e^- y / \sqrt{s}$)



Clear nuclear effects:
impulse approximation = scaled $\gamma + p$

Coherent diffraction, model comparison

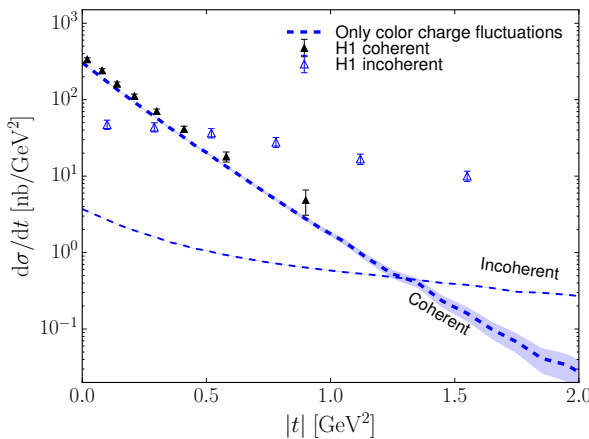


ALICE, 1305.1467

- nPDF (e.g. AB-EPS09) and saturation (LM-fIPSat) compatible
- Trivial $\gamma p \rightarrow \gamma A$ scaling clearly ruled out (AB-MSTW08)
- LHC UPC:
 - Limited to $Q^2 = 0$
 - No t spectra available (yet?)
 - Coherent-incoherent separation difficult

Applications of J/Ψ production 2: proton shape

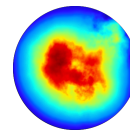
HERA data with only color charge fluctuations ($x \sim 10^{-3}$)



Recall

- Coherent \sim average
- Incoherent \sim fluct (variance)

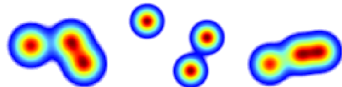
Round CGC proton:
Color charges + Yang-Mills



H.M, B. Schenke, 1607.01711, H1: 1304.5162

Constraining proton fluctuations

Simple constituent quark inspired picture:



- Sample quark positions from a Gaussian distribution (width B_{qc})
- Small- x gluons are located around the valence quarks (width B_q).
- Combination of B_{qc} and B_q sets the degree of geometric fluctuations

Proton = 3 overlapping hot spots

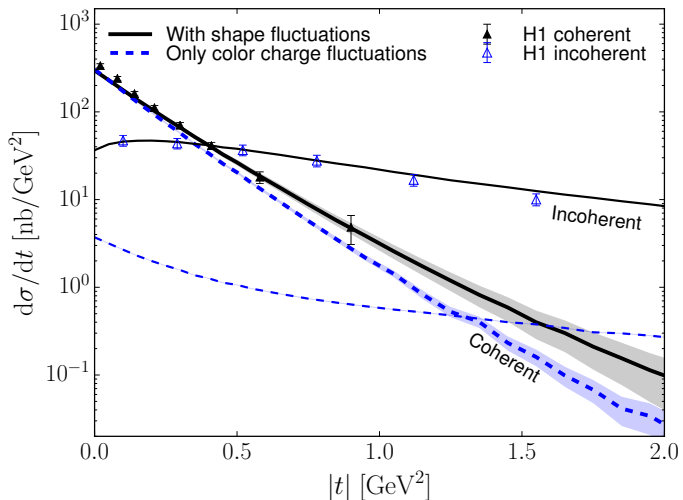
$$T_{\text{proton}}(b) = \sum_{i=1}^3 T_q(b - b_i) \quad T_q(b) \sim e^{-b^2/(2B_q)}$$

+ density fluctuations for each hot spot

H.M. Schenke, 1607.01711, 1603.04349, also more complicated geometries

Similar setup e.g. in Bendova, Cepila, Contreras; Cepila, Contreras, Krelina, Takaki; Traini, Blaizot

Constraining proton fluctuations: $\gamma + p \rightarrow J/\Psi + p$



HERA data requires large event-by-event fluctuations

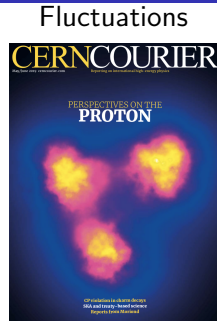
H.M. B. Schenke, 1607.01711

Heikki Mäntysaari (JYU)

Diffraction at EIC

September 25, 2019

8 / 20



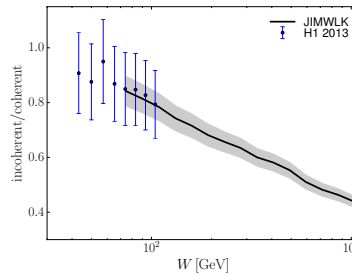
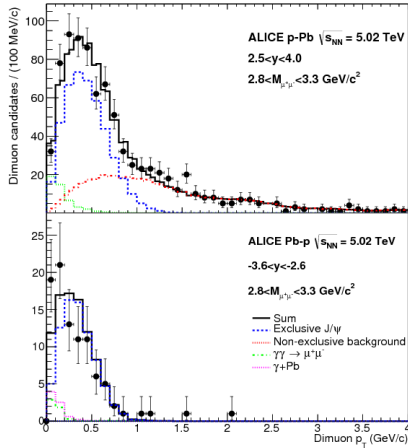
Energy dependence

ALICE measurement in $\gamma + p \rightarrow J/\Psi + p(p^*)$ collisions (p+Pb UPC)

$$x \sim 10^{-2} \rightarrow 2 \cdot 10^{-5}$$

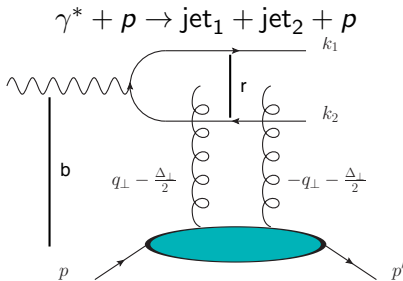
- Incoherent cross section ≈ 0 at small x
- Smoother proton (black disk) at small x ?

(Qualitatively) compatible with CGC evolution



Diffractive dijets: more differential imaging

Two momenta, extra handle



[Y. Hatta, B-W. Xiao, F. Yuan, 1601.01585](#)

$$d\sigma \sim v_0(1 + 2v_2 \cos[2\theta(\mathbf{P}, \Delta)])$$

- $\Delta = \mathbf{k}_1 + \mathbf{k}_2$ recoil momentum
- $\mathbf{P} = \frac{1}{2}(\mathbf{k}_1 - \mathbf{k}_2)$ dijet momentum
- Nearly back-to-back jets, $|\mathbf{P}| > |\Delta|$



[Hatta, Xiao, Yuan, 1601.01585](#)

[Hagiwara et al, 1706.01765](#)

v_2 in principle connected to elliptic part of gluon Wigner distribution in certain limit ($Q^2 \rightarrow 0$, $|\mathbf{P}| \gg |\Delta|$), in practice complicated

[H. M, N. Mueller, B. Schenke, 1902.05087:](#)

CGC calculation of dijet cross section and Wigner

Kinematics

EIC kinematics used here

- $Q^2 = 1\text{GeV}^2$
- $W = 100\text{GeV}$
- $|\mathbf{P}| = 1 \dots 3\text{GeV}$ (“mean jet p_T ”)
- $|\Delta| = 0.1\text{GeV}$ (recoil)
- $m_c = 1.4\text{GeV}$ (charm jets, avoid large dipoles)
- Longitudinal momentum fraction $z \in [0.1, 0.9]$

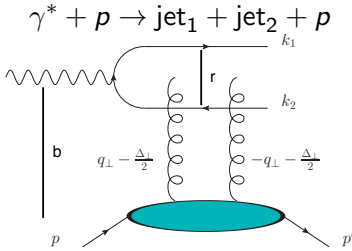
Fourier expansion in terms of $\theta(\mathbf{P}, \Delta)$:

Note: one may have $v_1 \neq 0$, depending on kinematics (backup!)



$$\Delta = \mathbf{k}_1 + \mathbf{k}_2, \mathbf{P} = \frac{1}{2}(\mathbf{k}_1 - \mathbf{k}_2)$$

CGC calculation for dijet production



Altinoluk, Armesto, Beuf, Rezaeian, 1511.07452

$$\frac{d\sigma}{d\mathbf{P} d\Delta} \sim \int_{\mathbf{b} \mathbf{b}' \mathbf{r} \mathbf{r}'} e^{-i(\mathbf{b}-\mathbf{b}') \cdot \Delta} e^{-i(\mathbf{r}-\mathbf{r}') \cdot \mathbf{P}} \mathcal{N}(\mathbf{r}, \mathbf{b}) \mathcal{N}(\mathbf{r}', \mathbf{b}') \otimes \dots$$

\mathbf{P} and Δ are conjugates to dipole size and impact parameter.

- Coordinate space:
Dipole amplitude $\mathcal{N}(\mathbf{r}, \mathbf{b})$ depends on $\theta(\mathbf{r}, \mathbf{b})$
- Momentum space:
Cross section depends on $\theta(\mathbf{P}, \Delta)$
- Mixed space:
Wigner distribution $xW(\mathbf{k}, \mathbf{b})$ depends on $\theta(\mathbf{k}, \mathbf{b})$

$$d\sigma \sim v_0(1 + 2v_2 \cos[2\theta(\mathbf{P}, \Delta)])$$

- $\Delta = \mathbf{k}_1 + \mathbf{k}_2$
- $\mathbf{P} = \frac{1}{2}(\mathbf{k}_1 - \mathbf{k}_2)$

Baseline study

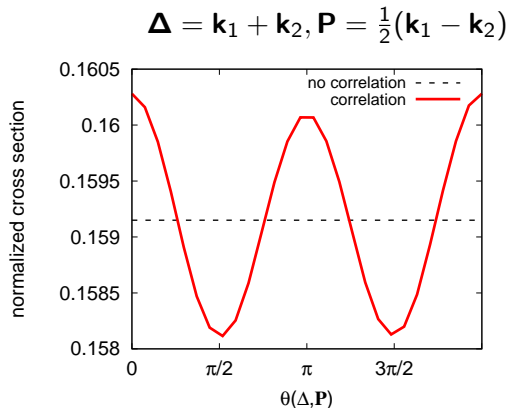
Introduce \mathbf{r}, \mathbf{b} correlation to the IPsat [Altinoluk, Armesto, Beuf, Rezaeian, 1511.07452](#)

Calculate two quark production (quark \approx jet)

$$N(\mathbf{r}, \mathbf{b}, x) = 1 - \exp \left[-\mathbf{r}^2 F(x, \mathbf{r}) T_p(\mathbf{b}) C_\theta(\mathbf{r}, \mathbf{b}) \right],$$
$$C_\theta(\mathbf{r}, \mathbf{b}) = 1 - \tilde{c} \left[\frac{1}{2} - \cos^2 \theta(\mathbf{r}, \mathbf{b}) \right]$$

$T(\mathbf{b})$: proton density profile

- $\tilde{c} = 0$: Standard IPsat (dashed)
- $\tilde{c} > 0$: Artificial dependence on $\mathbf{r} \cdot \mathbf{b}$
(solid line)



Dijet cross section has no dependence on $\theta(\mathbf{P}, \Delta)$ if $\tilde{c} = 0$ (dashed line)

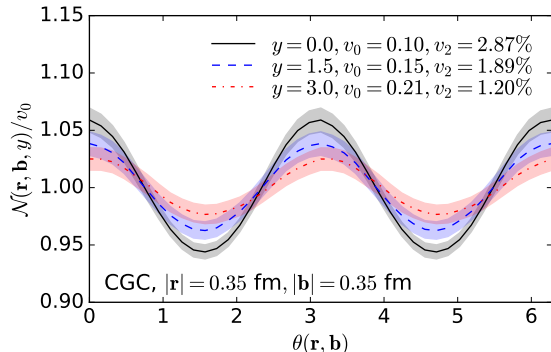
Realistic setup: angular correlations from CGC

Initial condition $x = 0.01$

- IPsat $Q_s^2(\mathbf{b}) \Rightarrow$ color charge density ρ
- MV model, local Gaussian $\langle \rho \rho \rangle \sim Q_s^2$
- Yang-Mills Eqs \Rightarrow Wilson lines $\Rightarrow \mathcal{N}$
- Infrared regulator: mass \tilde{m}

Small- x evolution

- JIMWLK equation
- Fixed and running coupling
- Infrared regulator: mass m



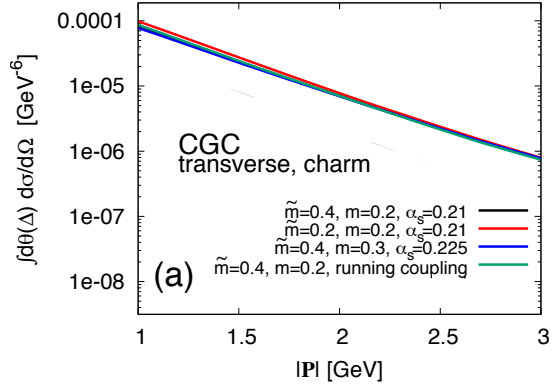
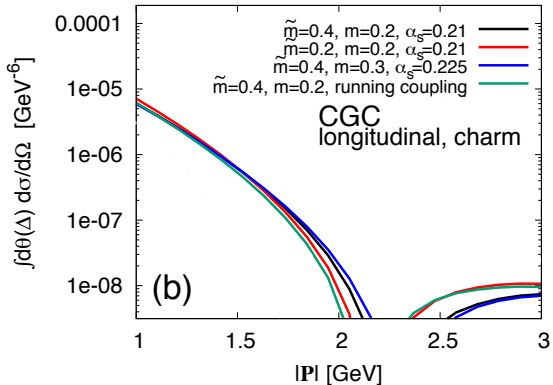
$$\mathcal{N}(\mathbf{r}, \mathbf{b}) = v_0(1 + 2v_2 \cos[2\theta(\mathbf{r}, \mathbf{b})])$$

Evolution suppresses elliptic modulation
Expect to see that also in dijet production

Parameters constrained by HERA F_2 and J/Ψ data

H.M, B. Schenke 1607.01711, 1806.06783

Charm dijets, dependence on dijet momentum $|\mathbf{P}|$ ($\gamma^* + p \rightarrow \text{jet} + \text{jet} + p$)

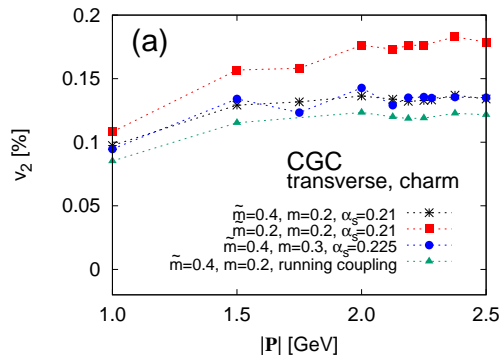
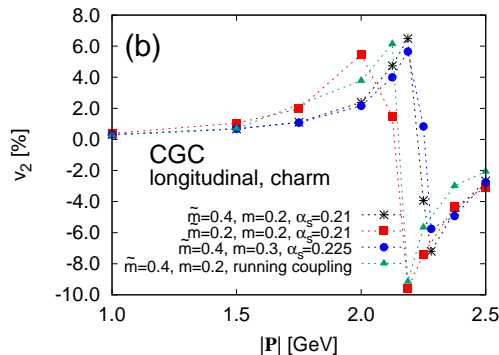


Transverse component dominates at $Q^2 = 1 \text{ GeV}^2$

Diffractive dips also in Δ spectra (not shown)

\mathbf{P} conjugate to dipole size \mathbf{r} , dip \sim size of the projectile $\sim 1/\sqrt{m_c^2 + z(1-z)Q^2}$

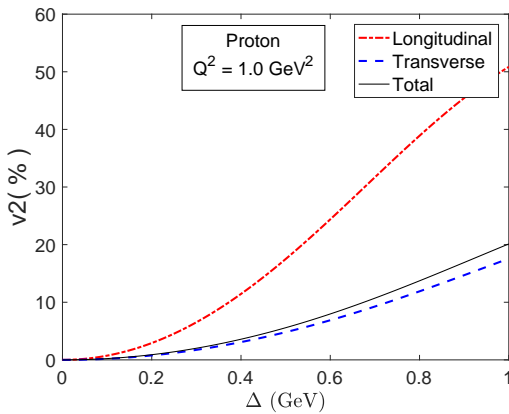
Charm dijets, extracted v_2 ($\gamma^* + p \rightarrow \text{jet} + \text{jet} + p$)



- Small sensitivity on IR regulators m, \tilde{m} and fixed/running α_s
- In this kinematics small modulation \sim few% (L) or $\sim 0.1\%$ (T, dominates)

$$d\sigma \sim v_0(1 + 2v_2 \cos[2\theta(\mathbf{P}, \Delta)])$$

Larger modulation away from correlation limit

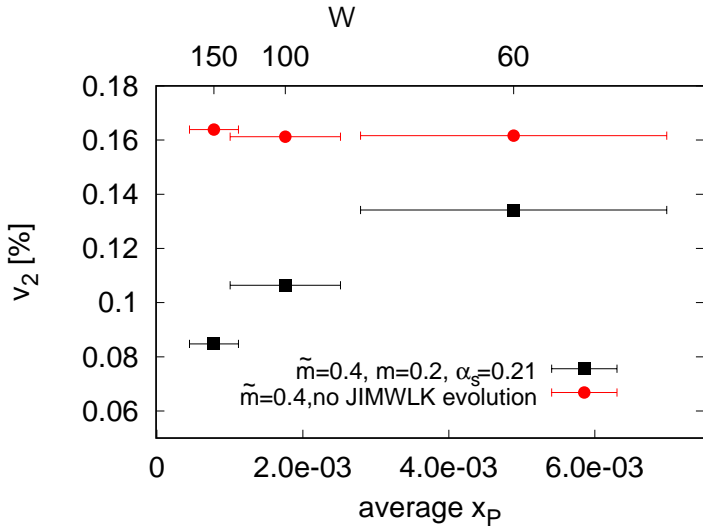


- Significant modulation at large $|\Delta|$
- ... where connection to Wigner is less clear
- But can calculate σ and Wigner from CGC [H. M, N. Mueller, B. Schenke, 1902.05087](#)
- Similar result in calculation including soft gluon radiation in the final state

[Hatta, Mueller, Ueda, Yuan, 1907.09491](#)

Salazar, Schenke, [1905.03763](#)

Energy dependence of total v_2 (transverse + longitudinal)



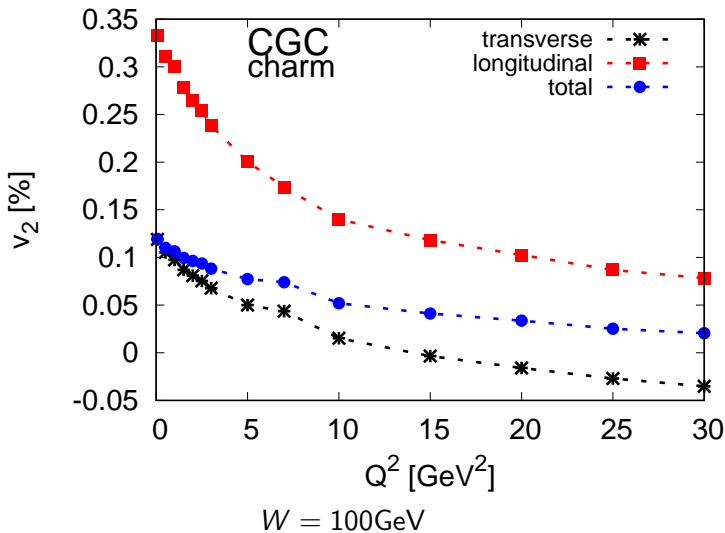
With JIMWLK

- v_2 decreases by factor ~ 2 in the EIC energy range
- Dominant reason: proton grows
→ Smaller density gradients
- Similar growth seen in J/ψ spectra at HERA

No JIMWLK:

- No energy dependence

Q^2 dependence



- Large $Q^2 \Rightarrow$ smaller dipoles sensitive to smaller density gradients
- Transverse v_2 can become negative at large Q^2

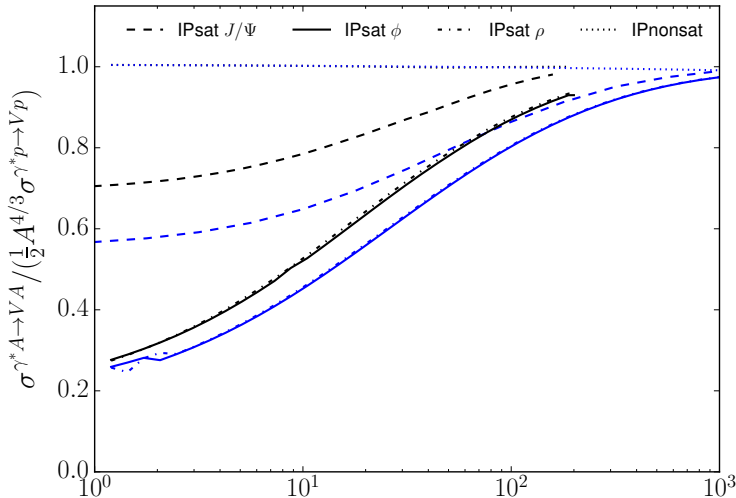
Conclusions

- Exclusive vector meson production is powerful
 - Sensitivity on small- x gluons
 - Access to geometry
 - Access to fluctuations
 - Need coherent – incoherent separation
- Dijet production: extra handle more detailed imaging
- Angular modulation in the cross section:
Intrinsic impact parameter-transverse momentum correlations in the gluon distribution
- Predict angular modulation at the EIC for charm dijets from CGC
 - And energy and Q^2 dependence
 - Small modulation $\sim 0.1 \dots 1\%$ close to correlation limit
 - Larger away from the correlation limit
- Also in [1902.05087](#) and backup: Calculated Wigner and Husimi distributions describing small- x gluons from CGC
 - Elliptic modulation of these distributions \sim dijet v_2
- Work in progress: incoherent dijet production

BACKUPS

Large nuclear suppression in vector meson production

$W = 100, 1000 \text{ GeV}$



Diffractive dijets: more differential imaging

The most complete description of the partonic structure

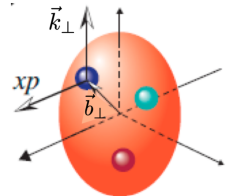
$$W(x, \vec{k}_\perp, \vec{b}_\perp) = \int \frac{d^2\Delta_\perp}{(2\pi)^2} e^{i\vec{b}_\perp \cdot \vec{\Delta}_\perp} \int \frac{dz^- d^2 z_\perp}{16\pi^3} e^{ixP^+ z^- - i\vec{k}_\perp \cdot \vec{z}_\perp} \langle P - \frac{\Delta}{2} | \bar{q}(-z/2) \gamma^+ q(z/2) | P + \frac{\Delta}{2} \rangle$$

$\int d\vec{b}_\perp$ ↓ $\int d\vec{k}_\perp$

TMD $f(x, \vec{k}_\perp)$ GPD $f(x, \vec{b}_\perp)$ $\int dx$

$\int d\vec{k}_\perp$ ↓ $f(x)$ $\int d\vec{b}_\perp$ $F(\vec{b}_\perp)$ Form factor

PDF $\int dx$ Q charge $\int d\vec{b}_\perp$



Graphics from Y. Hatta

Wigner and Husimi distributions – to the mixed space

Compare predicted dijet v_n to gluon Wigner and Husimi distributions [Hagiwara, Hatta, Ueda, 1609.05773](#)

Wigner distribution $xW(x, \mathbf{P}, \mathbf{b})$

- Most complete description
- No probabilistic interpretation (uncertainty principle)
- Not positive definite
- Large dipoles important

Husimi distribution $xH(x, \mathbf{P}, \mathbf{b})$

- Wigner + with Gaussian smearing
- Positive definite, probabilistic interpretation
- Dependence on the smearing parameter $\textcolor{blue}{l}$
- Large dipoles suppressed by $\textcolor{blue}{l}$

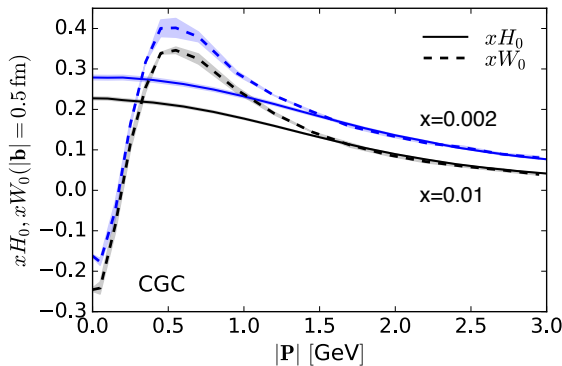
$$xW(x, \mathbf{P}, \mathbf{b}) = \frac{-2N_c}{(2\pi)^2 \alpha_s} \int_{\mathbf{r}} e^{i\mathbf{P} \cdot \mathbf{r}} \left(\frac{1}{4} \nabla_{\mathbf{b}}^2 + \mathbf{P}^2 \right) \mathcal{N}(\mathbf{r}, \mathbf{b}, x) = xW_0 + 2xW_2 \cos[2\theta(\mathbf{P}, \mathbf{b})].$$

$$xH(x, \mathbf{P}, \mathbf{b}) = \frac{1}{\pi^2} \int_{\mathbf{b}' \mathbf{P}'} e^{-(\mathbf{b}-\mathbf{b}')^2/\textcolor{blue}{l}^2 - (\mathbf{P}-\mathbf{P}')^2} xW(x, \mathbf{P}', \mathbf{b}') = xH_0 + 2xH_2 \cos[2\theta(\mathbf{P}, \mathbf{b})]$$

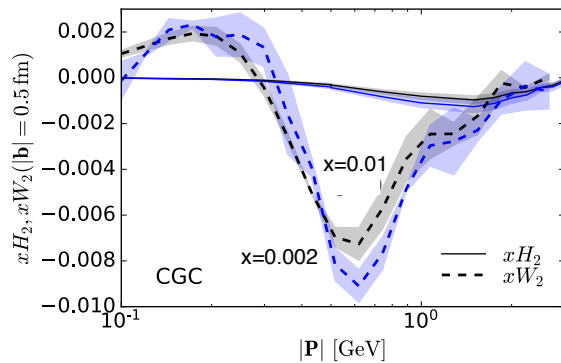
Here $\textcolor{blue}{l} = 1\text{GeV}^{-1}$ corresponds to coordinate space smearing distance $\sim 0.2 \text{ fm}$

Wigner and Husimi distributions - to the mixed space

$$xH = xH_0 + 2xH_2 \cos 2\theta(\mathbf{P}, \mathbf{b}), xW = xW_0 + 2xW_2 \cos 2\theta(\mathbf{P}, \mathbf{b})$$



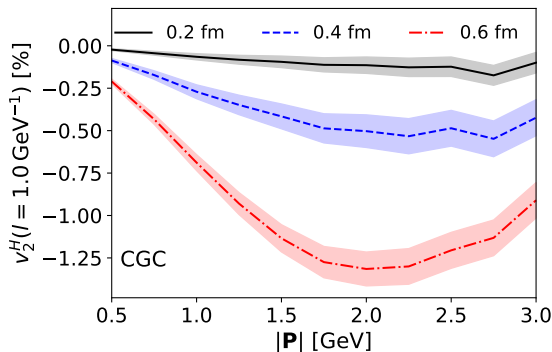
- Wigner distribution negative at small $|\mathbf{P}|$
- At $|\mathbf{P}| \gtrsim 1/\textcolor{blue}{l}$ matches Husimi



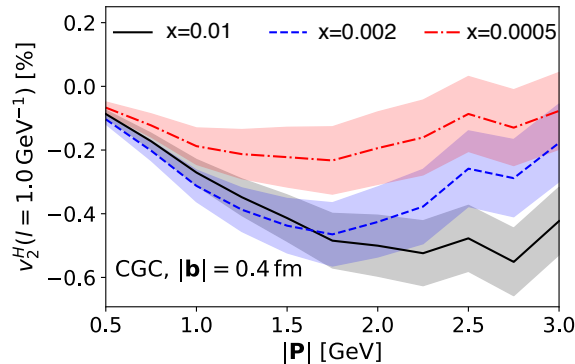
- Elliptic parts negative, match at $|\mathbf{P}| \gtrsim 1/\textcolor{blue}{l}$
- $|xW_2| \gg xH_2$ at small $|\mathbf{P}|$

Husimi distribution, closer look

Study Husimi distribution and define $v_2^H = x\mathbf{H}_2/x\mathbf{H}_0$, find $v_2^H \sim 0.1\dots 1\% \sim$ dijet v_2



- Large ellipticity at large impact parameters
- $v_2^H \rightarrow 0$ at large $|\mathbf{P}|$: target smooth at small distance scales

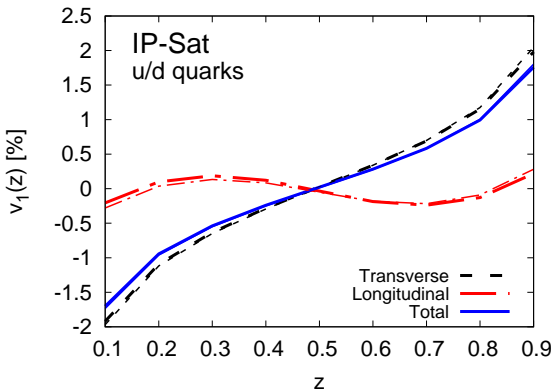


- Generally $v_2^H \rightarrow 0$ due to evolution
- Increasing $|v_2^H|$ at small $|\mathbf{P}|$: proton grows, and gradients at scale $\sim l$ start to contribute

Isolating kinematical effects effects

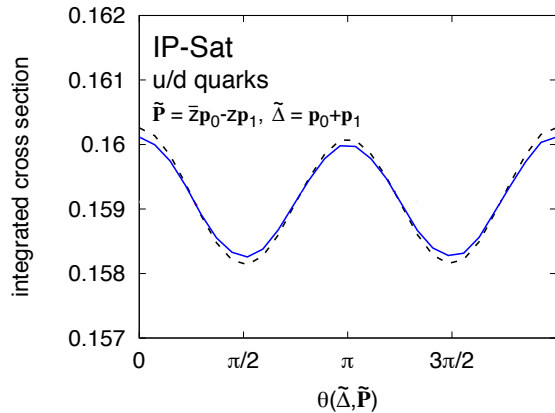
$$\Delta = \mathbf{k}_1 + \mathbf{k}_2, \mathbf{P} = \frac{1}{2}(\mathbf{k}_1 - \mathbf{k}_2)$$

- Probed $x_{\mathbf{P}}$ depends on $\theta(\mathbf{P}, \mathbf{b}) \Rightarrow v_1 \neq 0$
- Vanishes if $z_{\min} = 1 - z_{\max}$

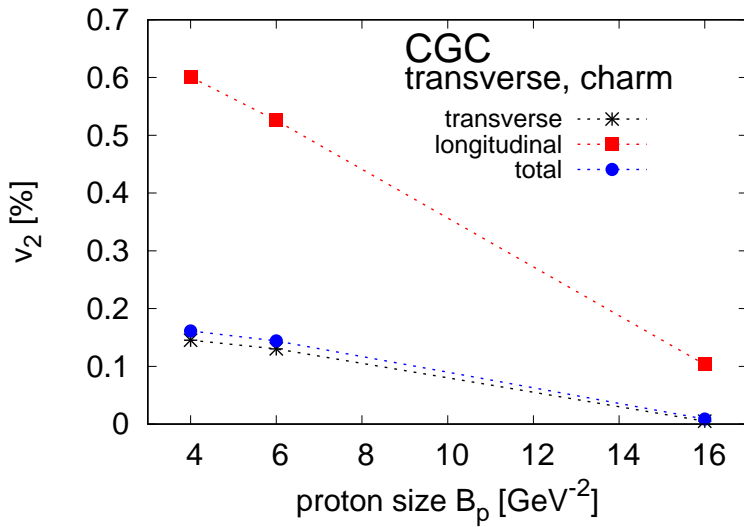


Alternative: $\tilde{\mathbf{P}} = (1 - z)\mathbf{k}_1 - z\mathbf{k}_2$ [Dumitru et al, 2018](#)

- $x_{\tilde{\mathbf{P}}}$ independent of $\theta(\mathbf{P}, \mathbf{b})$, no v_1
- $v_2 \neq 0$ with no correlations in IPsat



Proton size dependence



Total cross section

